MRO (CRISM/MARCI) MAPPING OF THE SOUTH POLE – FIRST MARS YEAR OF OBSERVATIONS.

A. J. Brown[1], W.M. Calvin[2] and S.L. Murchie[3] [1]SETI Institute, 515 N. Whisman Rd Mountain View, CA 94043, abrown@seti.org., [2]Geological Sci. & Eng., University of Nevada, Reno, NV, 89557, [3]JHU APL, Laurel, MD 20723. Author website: http://abrown.seti.org

Introduction: We report on mapping of the south polar region of Mars with the CRISM imaging spectrometer Multi-Spectral Polar (MSP) dataset [1]. Our observations suggest these new discoveries:

1. Water ice is present in the form of pole-circling clouds originating from the circum-Hellas region, beginning prior to L_s=162 and diminishing markedly at L_s=200-204 (Figure 1).

2. Surface water ice that is present in the final stages of sublimation [2,3] is present in the 'cryptic region', and some small areas outside the traditional cryptic region that may share similar characteristics (for example, the western slope of Lau crater). Some of this water ice is 'pure' in the sense that CRISM resolves only water ice and not a CO_2-H_2O ice mixture. This water ice quickly sublimes completely by L_s=252 and may be the source of water vapor observed by CRISM in southern latitudes between L_s=240-260 [4].

3. Large grained CO_2 ice is present in the south polar residual cap and gets progressively finer grained as sublimation proceeds throughout spring. We have estimated seasonal surface CO_2 ice grain size distributions (or equivalent path lengths) and our model suggests that grain sizes peak at L_s=191-199, with CO_2 grain sizes of 5cm not unusual on the residual cap.

CRISM: The Compact Reconnaissance Imaging Spectrometer for Mars (CRISM) is a visible to near-infrared spectrometer sensitive to photons with wavelengths from ~0.4 to ~4.0μm [5]. In high-resolution mode, CRISM's instantaneous field of view (pixel) size corresponds to ~18.75m on the ground. CRISM has 640 pixels in the FOV, however only 605 see the surface, therefore the swathe width covers ~10.8km on the ground. In mapping mode (primarily used in this study) 10x binning is employed in the cross-track direction, therefore a mapping swathe has 60 pixels covering approximately 10.8km on the surface. Along-track binning is controlled by exposure time.

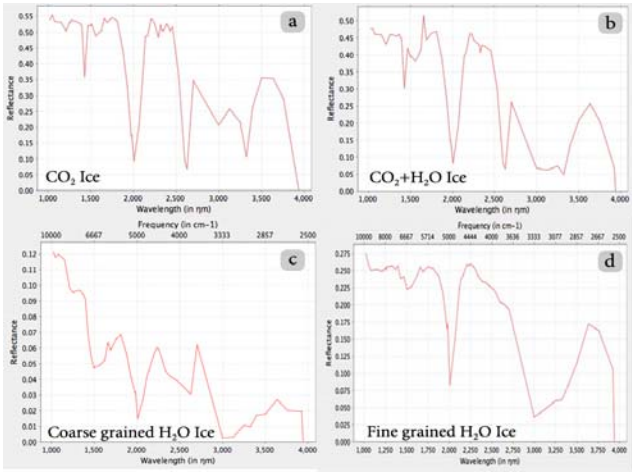

Figure 1. Example CRISM MSP 55 band L-channel spectra used in mapping icy volatiles in the south polar regions. These spectra have been corrected for the incidence angle of the sun on the surface but no atmospheric correction has been applied.

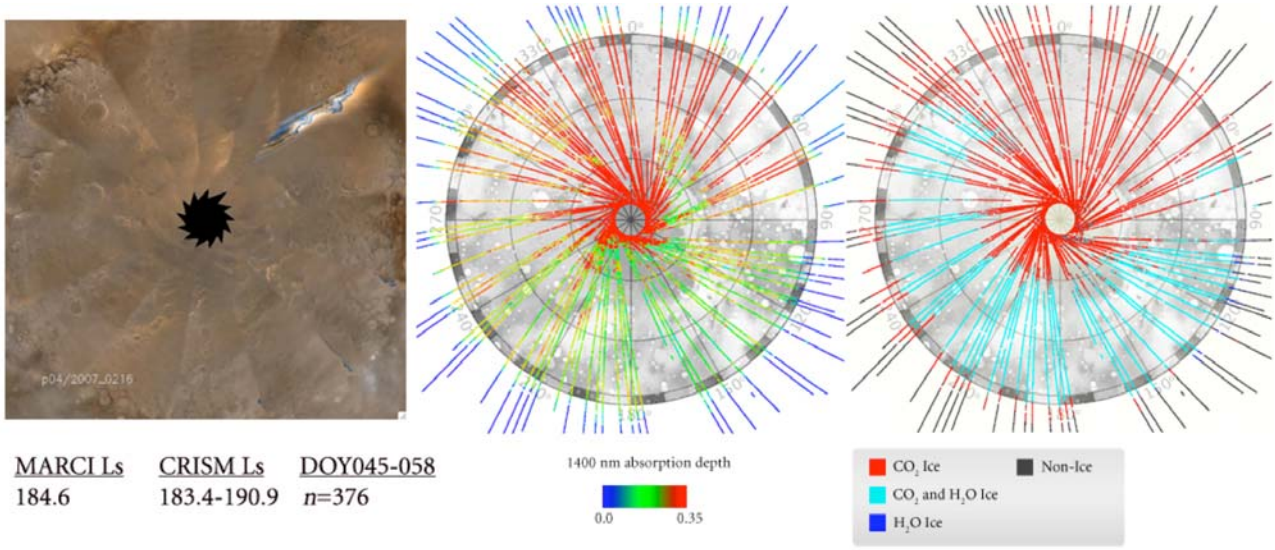

Figure 2. One exmaple of the MRO south polar mapping sequence showing MARCI daily map, CO_2 absorption band map and derived icy volatile map for L_s=183.4-190.9. Note presence of H_2O ice cloud almost completely encircling the pole at this time (in cyan on rightmost image).

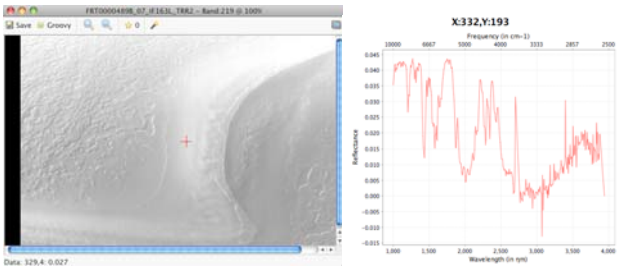

Figure 3. CRISM observation FRT489B (281.7E, 87S @ L_s=190), and an example spectra of coarse grained CO_2 ice (taken from the point beneath the red cross). The 55% band depth of this spectrum indicates grain sizes in excess of 5cm (see text).

MARCI: The MARs Color Imager (MARCI) camera is a super wide angle, fish eye lens instrument with 1024 pixels-wide CCD. As the name implies, it obtains 12 continuous terminator-to-terminator, limb-to-limb color images, 60° of longitude wide every day. The instruments seven bandpass filters are positioned at 260, 320 (UV), 425, 550, 600, 650 and 725nm(VIS). The UV channels have 7-8km resolution and the VIS channels just under 1km resolution [6]. We produced images using MARCI daily global maps projected to polar stereographic projection.

Grain size mapping: We have constructed grain size maps by two methods – using the 1.435 μm absorption band depth and a combination of the 2.18 and 2.34 μm CO_2 absorption bands, as recommended by [8]. The latter method avoids the affects of CO_2 gas bands, however in mapping mode, the CRISM smile complicates interpretation of these small features on the edge of the image. Figure 3 shows an example of coarse grain CO_2 ice in the Swiss cheese terrain at 281.7E, 87S at L_s=190, the start of spring. A simple

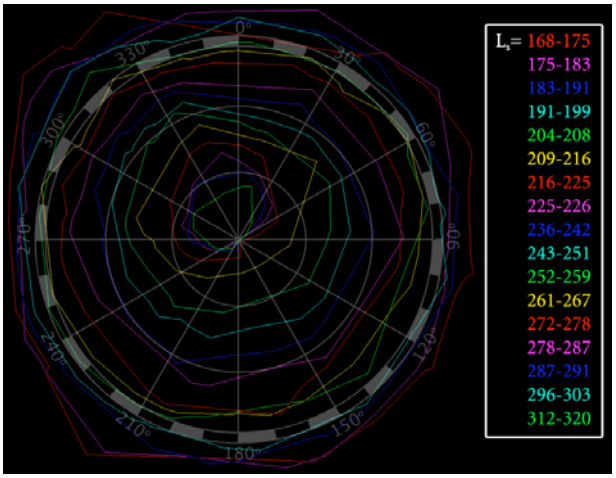

Figure 4. CROCUS (Cap Recession Observations indicated CO2has Ultimately Sublimated [7]) line vs. solar longitude during springtime recession for MY 28.

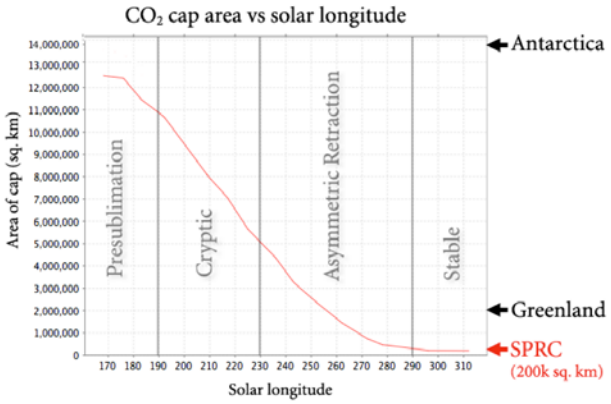

Figure 5. Cap area and sublimation phase vs. solar longitude during springtime recession for MY 28 as determined by CRISM icy volatiles mapping.

Shkuratov model of pure CO_2 ice indicates grain sizes of at least 5cm are required to replicate this feature. We are revising Fig. 9 of [8] to reflect CO_2 optical constants that have been published since, e.g. [9].

CROCUS Mapping: We calculated the CROCUS line using the icy volatile mosaics (Figure 4-5). We defined the edge of the retreating cap as the location where CO_2 or CO_2+H_2O was found, furthest away from the south pole. Due to the patchy nature of CRISM MSP coverage, we used a computer algorithm to automatically recognize the edge of the cap by laying down transects away from the pole, and finding the point along that transect where the last CO_2 or CO_2+H_2O point was mapped. In order to avoid outliers or spurious noise, for the detection of the cap edge we required that the pixel in question must be surrounding by five adjacent pixels that were also mapped as containing CO_2 or CO_2+H_2O ice. We used linear interpolation to jump over areas of missing data. We used a variable lookahead scheme to look for the next point with the greatest radius away from the south pole. Surface areas were calculated using a Mars spheroid with no topography and employing a Monte Carlo routine to assess polygon areal coverage in latitudinal bands.

Acknowledgements: We would like to thank the CRISM team at APL and the MARCI team at MSSS led by Mike Malin for producing these excellent Martian datasets.

References: [1] Brown, A.J. et al. 2009. *JGR* submitted [2] Titus, T. et al. 2003, *Science* 299, 1048-1051 [3] Langevin, Y. et al. 2007, *JGR* 112, doi:10.1029/2006JE002841 [4] Smith, M.D. et al., 2009, *JGR* submitted [5] Murchie, S. et al. (2007) *JGR* 112, doi:10.1029/2006JE002682 [6] Malin et al. 2001 *JGR* 106, 17651-17672 [7] Kieffer, H. et al. 2000 *JGR* 105, 9653-9699 [8] Calvin, W. and Martin, T. (1994) *JGR* 99 21143-21152 [9] Hansen, G. (1997) *JGR* 102 21569-21587.